Available online at www.derpharmachemica.com

Scholars Research Library

Der Pharma Chemica, 2015, 7(10):237-245
(http://derpharmachemica.com/archive.html)

ISSN 0975-413X
CODEN (USA): PCHHAX

Theoretical prediction and experimental study of 5-methyl-*1H*-pyrazole-3-carbohydrazide as a novel corrosion inhibitor for mild steel in 1.0 M HCl

H. Elmsellem[1*], K. Karrouchi[1,2], A. Aouniti[1], B. Hammouti[1], S. Radi[1], J. Taoufik[2], M. Ansar[2] , M. Dahmani[1,3], H. Steli[4] and B. El Mahi[1]

[1]Laboratoire de Chimie Appliquée et environnement (LCAE-URAC18), Faculté des Sciences, Oujda, Maroc
[2]Laboratoire de Chimie Thérapeutique, Faculté de Médecine et de Pharmacie, Université Mohammed V de rabat, Maroc
[3]LCOMPN-URAC25, Faculté des Sciences, Université Mohammed Premier, Oujda, Morocco
[4]Laboratoire mécanique & énergétique, Faculté des Sciences, Université Mohammed Premier, Oujda, Morocco

---

ABSTRACT

This work is devoted to examine the effectivenes of 5-methyl-1H-pyrazole-3-carbohydrazide(MPC) on corrosion of mild steel in 1 M HCl solution using the weight loss measurement at various temperature and concentration effects. Polarization curves and electrochemical impedance spectroscopy (EIS) methods were employed to evaluate corrosion rate and inhibition efficiency. Inhibition efficiency of ***95%*** *is reached with* 10^{-3} *M of* ***(****MPC****)*** *at* ***308*** *K. Potentiodynamic polarization showed that the MPC behaves as mixed-type inhibitor. The Nyquist plots showed that increasing MPC concentration, charge-transfer resistance increased and double-layer capacitance decreased, involving increased inhibition efficiency. Adsorption of the inhibitor molecules corresponds to Langmuir adsorption isotherm. Quantum chemical calculations showed that the inhibitor has the tendency to be protonated in the acid and the results agree with experimental observations.*

Key words: Mild Steel, HCl, Corrosion inhibition, MPC, Weight loss, Electrochemical, DFT method

---

INTRODUCTION

The many interesting properties of mild steel and its alloy (well as low cost) have endeared the metal to be utilized in various industrial applications. However, these properties are lost to corrosion when the metal is deployed in long term service in a corrosive environment. Therefore, it is imperative for the metal to be protected against corrosion when intended for use in such an environment. Several approaches have been employed toward boosting the corrosion resistance ability of mild steel [1]

The corrosion of metals, including mild steel, is a serious problem in many industries, especially during processes such as the pickling of steel, acid washing and etching [2, 3]. The study of corrosion processes and their inhibition by organic inhibitors is a very active field of research [4]. Many researchers report that the inhibition effect mainly depends on some physicochemical and electronic properties of the organic inhibitor which relate to its functional groups, steric effects, electronic density of donor atoms, and orbital character of donating electrons, and so on [5, 7]. Among numerous inhibitors, N-heterocyclic compounds are considered to be the most effective corrosion inhibitors [10]. Up to now, various N-heterocyclic compounds are reported as good corrosion inhibitors for steel in acidic media, such as pyrazole derivatives [8–10], bipyrazole derivatives [11, 12]. As another important kind of N-heterocyclic compound, pyrazine derivatives whose molecules possess the pyrazine ring with two N heteroatoms could also be seemed as good potential inhibitors. However, data regarding the use of pyrazine derivatives as corrosion inhibitors is very scarce. Hammouti et al. [13, 14] studied the inhibition effect of diethyl pyrazine-2,3-

dicarboxylate on the corrosion of steel in 0.5 M H_2SO_4, and its maximum inhibition efficiency (E) was about 82% at 0.01 M. As ordinary pyrazine derivatives, 2-methylpyrazine (MP, $C_5H_6N_2$), 2-aminopyrazine (AP,$C_4H_5N_3$) and 2-amino-5-bromopyrazine (ABP, $C_4H_4N_3Br$) have good solubility in water, and are widely used as intermediates for the preparation of drugs. According to our recent work [15], the pyrazine derivatives of AP and ABP act as good corrosion inhibitors on the corrosion of steel in 1.0 M HCl, which incite us to further extend the corrosion inhibition by auther pyrazine derivatives for mild steel in 1M HCl.

Accordingly, the aim of this work is to study the inhibition action of 5-methyl-1H-pyrazole-3-carbohydrazide(**MPC**), on the corrosion of mild steel in 1M HCl. The inhibition performance is evaluated by weight loss, electrochemical impedance spectroscopy (EIS) and potentiodynamic polarization measurements, complemented with quantum calculations.

MATERIALS AND METHODS

2.1. Materials and solutions

2.1.1. Inhibitor

Figure1 shows the molecular structure of the investigated compound\ which has been labelled **MPC**.

2.1.2. General procedure for the preparation of 5-methyl-1H-pyrazole-3-carbohydrazide(MPC)

To a solution of 5-methyl-1H-pyrazole-3-carbohydrazide (1 mmol) in 10 ml of ethanol, it was added an equimolar amount of 2-chlorobenzaldehyde derivative in the presence of acetic acid. The mixture was maintained under reflux for 2 h, until TLC indicated the end of reaction. Then, the reaction mixture was poured in cold water, and the precipitate formed was filtered out washed with ethanol.

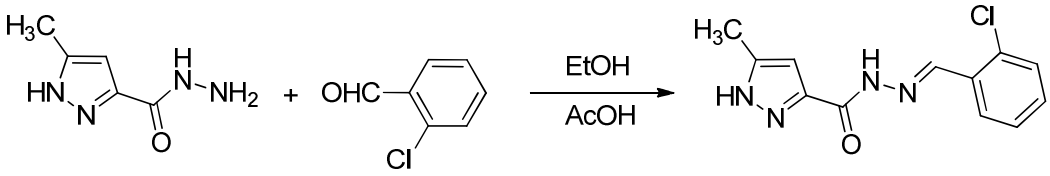

Figure 1. Synthesis and characterization of N'-(2-chlorobenzylidene)-5-methyl-1H-pyrazole-3-carbohydrazide(MPC) .

Yield 78%. IR (ν(cm^{-1})) : 3182 (NH), 1665 (C=O), 1552 (N=CH).^{1}H NMR: (300MHz, DMSO-d_6, δ(ppm)) : 2.27 (s, 3H, CH_3), 6.49 (s, 1H, CH-Pz), 7.39-7.99 (m, 4H, H-Ar), 8.90 (s, 1H, N=CH), 11.92 (s, 1H, NHCO), 13.09 (s, 1H, NH-Pz). ^{13}H NMR: (300MHz, DMSO-d_6, δ (ppm)): 10.77, 105.40, 127.31, 128.01, 130.34, 131.70, 132.41, 133.57, 140.56, 143.65, 146.16, 159.05.ESI-MS: m/z = 263.1 $[M-H]^+$.

2.1.3. Solution

The aggressive solutions of 1.0 M HCl were prepared by dilution of an analytical grade 37% HCl with double distilled water. The concentration range of green inhibitor employed was 10^{-3} – 10^{-6} (M).

RESULTS AND DISCUSSION

3.1 Weight Loss Measurements

Corrosion of mild steel in 1 M HCl containing different concentrations of MPC was studied by weight loss measurements, that is, measuring the mass of metal turned into corrosion products per unit area of surface per unit of time.

The corrosion rate (ρ) in mg cm-2 h-1 in the absence and presence of ‘‘MPC’’ was determined using the following equation:

$$\rho = \frac{\Delta W}{At} \qquad \textbf{(1)}$$

where ΔW is the average weight loss of the mild steel specimens, A is the total area of mild steel specimen and t is the immersion time. The percentage inhibition efficiency (E%) was calculated using the relationship:

$$Ew\ (\%) = \frac{W0 - Wi}{W0} \text{x } 100 \qquad \textbf{(2)}$$

Where Wo and Wi are the weight loss values in the absence and presence of ‘‘MPC’’.

At this point it is worth mentioning that all data presented below in Figures and Tables related to corrosion rate and inhibition efficiency, were calculated from weight loss measurements.

Table 1. weight loss mesurements of different concentration with and without presence of MPC

Compound	C	w (mg/cm².h)	Ew %
Blank	1M	0.8200	_
Inhibitor ''MPC''	10^{-6}	0.1733	79
	10^{-5}	0.0917	89
	10^{-4}	0.0658	92
	10^{-3}	0.0431	**95**

3.2. Adsorption isotherm

Organic inhibitors exhibit inhibition ability via adsorption on the solution/metal interface, while the adsorption isotherm can provide the basic information about the interaction between the inhibitor and the metal surface [16, 17]. We tested various adsorption isotherms to fit the experimental data, such as Langmuir, Temkin and Frumkin adsorption isotherms. For **MPC**, the plot of C versus C/θ yield sastraight line with slope nearly 1 and the linear association coefficient (R^2) is also nearly 1 (Fig.2), showing that the adsorption of **MPC** on the carbon steel surface can be well described by Langmuir adsorption isotherm: Eq.(3). This kind of isotherm involves the single layer adsorption characteristic and no interaction between the adsorbed inhibitor molecules on the carbon steel surface [18, 19].

$$\frac{C}{\theta} = \frac{1}{\mathrm{K}} + C \qquad (3)$$

Where C is the concentration of inhibitor, K the adsorption equilibrium constant, and Ɵ is the surface coverage.

The constant of adsorption, K_{ads}, is related to the standard free energy of adsorption, $\Delta \mathbf{G}^{\circ}_{ads}$, with the following equation:

$$\Delta G^{\circ}_{ads} = -RT.ln(55{,}5.K) \qquad \mathbf{(4)}$$

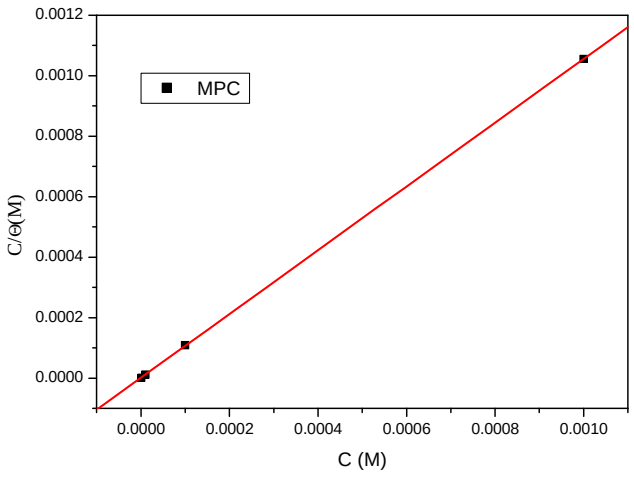

Figure 2. Langmuir adsorption of MPC on the midl steel surface in 1.0 M HCl solution

The thermodynamic parameters for the adsorption process were obtained from this figure are shown in Table 2.

Table 2. Thermodynamic parameters for the adsorption of MPC in 1.0 M HCl on the carbon steel at 308K

Inhibitor	K_{ads} L mol^{-1}	ΔG_{ads} kJ mol^{-1}	Linear coefficient regression (r)
''MPC''	743621.58	-44.88	1.05432

The value of ΔG°_{ads} is negative which indicate that these investigated compound is strongly adsorbed on the carbon steel surface and show the spontaneity of the adsorption process and stability of the adsorbed layer on the carbon steel surface. Generally, values of ΔG°_{ads} up to -20 kJ mol^{-1} are consistent with the electrostatic interaction between the charged molecules and the charged metal (physical adsorption) while those more negative than -40 kJ mol^{-1} involve sharing or transfer of electrons from the inhibitor molecules to the metal surface to form a coordinate type of bond (chemisorption) [20]. It can be assumed that the adsorption of **MPC** on mild steel surface occurs first due to electrostatic interaction, and then the desorption of water molecules is accompanied by chemical interaction between the adsorbate and metal surface [21].

3.3. Electrochemical measurements

The electrolysis cell was Pyrex of cylinder closed by cap containing five openings. Three of them were used for the electrodes. The working electrode was mild steel with the surface area of 1 cm^2. Before each experiment, the electrode was polished using emery paper until 1200 grade. After this, the electrode was cleaned ultrasonically with distillate water. A saturated calomel electrode (SCE) was used as a reference. All potentials were given with reference to this electrode. The counter electrode was a platinum plate of surface area of 1 cm^2. The temperature was thermostatically controlled at 308 K. The working electrode was immersed in test solution during 30 minutes until a steady state open circuit potential (Eocp) was obtained. The polarization curve was recorded by polarization from -800 mV to -200 mV under potentiodynamic conditions corresponding to 1mV/s (sweep rate) and under air atmosphere.

The potentiodynamic measurements were carried out using VoltaLab100 electrochemical analyzer, which was controlled by a personal computer. AC-impedance studies also were carried out in a three electrode cell assembly. The data were analyzed using Voltamaster 4.0 software. The electrochemical impedance spectra (EIS) were acquired in the frequency range 100 kHz to 10 mHz at the free corrosion potential. The charge transfer resistance (R_{ct}) and double layer capacitance (C_{dl}) were determined from Nyquist plots. The impedance diagrams are given in the Nyquist representation. Experiments are repeated three times to ensure the reproducibility. All electrochemical studies were carried out with immersion time of 1 hour, with different inhibitory concentrations of **‘‘MPC’’**, at 308 K.

3.3.1. Open circuit potential (OCP)

Fig. 3 shows the time evolution of the OCP for the mil steel/blank solution interface at (308 ± 1) K. The blank solution is the most corrosive among the tested solutions and consequently the most demanding in terms of attaining stable steady-state conditions. It can be observed that after 30 min of immersion time t only negligible changes in the OCP are measured.

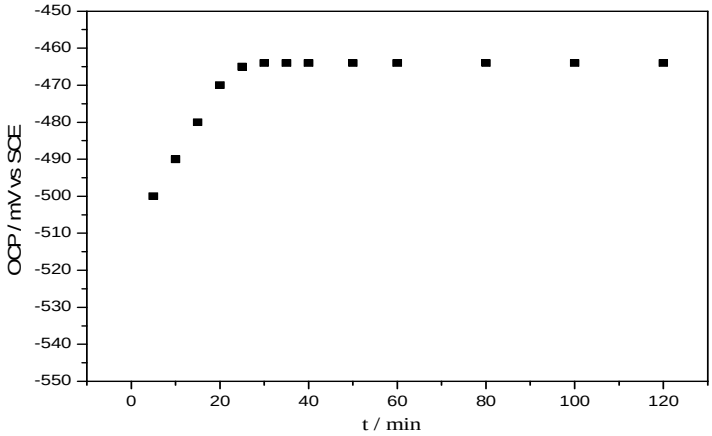

Figure 3. Time evolution of the OCP for the steel/blank solution interface at (308 ± 1) K

3.3.2. Potentiodynamic polarization

Polarization curves for the mild steel in 1 M HCl in the absence and presence of different concentrations of pyrazine derivative are shown in Fig. 4. The corresponding electrochemical parameters including corrosion potential (E_{corr}), Tafel slope (βc), corrosion current density (I_{corr}) and inhibition efficiency (Ep) are given in table 3. Clearly, upon increase of the inhibitor, both βa and βc values varied accordingly and the Icorr values decreased prominently. This means that both anodic metal dissolution of iron and cathodic hydrogen evolution reaction were inhibited. Moreover, the Ep values obtained from Tafel extrapolation are in good agreement with those obtained from impedance methods. The corrosion potential of mild steel shifted 2–23 mV with respect to that of the blank, which

suggests that **MPC** behaves as a mixed-type corrosion inhibitor for mild steel [22, 23] by first adsorbing on the metal surface and then blocking the reaction sites of the metal surface without affecting the anodic and cathodic reaction [24].

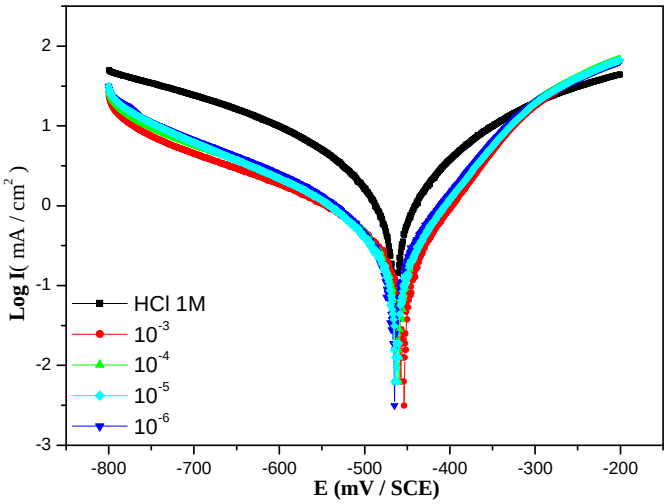

Figure 4. Polarization curves for mild steel in 1 M HCl in the absence and presence of various concentrations of inhibitor MPC

Table 3. Electrochemical parameters obtained from polarization curves for mild steel in 1 M HCl containing various concentrations of MPC at 308 k

Inhibitor	C (M)	$-E_{corr}$ (mV)	I_{corr} ($\mu A/cm^2$)	-βc (mV/dec)	βa (mV/dec)	Ep(%)
1M HCl	-	464	1386	184	135	--
‘‘MPC’’	10^{-6}	459	279	123	73	80
	10^{-5}	463	258	139	75	81
	10^{-4}	466	151	142	76	89
	10^{-3}	455	112	154	69	**92**

3.3.3. Electrochemical impedance spectroscopy (EIS) measurements

The Nyquist plots obtained for mild steel in 1 M HCl in the absence and presence of various concentrations of the **MPC** is shown in Fig. 5.These plots were characterized by one depressed semi-circular capacitive loop at high frequency, which is then followed by one small inductive loop at low frequency. The impedance spectra present an almost perfect semicircle, the center of which lies under the real axis. Such phenomena often refer to the frequency dispersion of interfacial impedance, which has been attributed to the roughness, or inhomogeneity, of the solid surfaces and adsorption of inhibitors [25]. Therefore, a constant phase element (CPE) is used instead of a capacitive element to obtain a more accurate fit of our experimental data sets, using generally more complicated equivalent circuits. The CPE impedance is given by [26]:

$$\mathbf{Z_{CPE} = A^{-1} (\mathit{iw})^{-n}} \qquad \mathbf{(5)}$$

In this equation, A is the CPE constant, *w* is the angular frequency (in rad s^{-1}), $i^2 = -1$ (the imaginary number) and n is a CPE exponent that can be used as a gauge of the heterogeneity, or roughness, of the surface. The equivalent circuit model employed for this system is shown in Fig. 6 and consists of an uncompensated solution resistance Ru in series to the parallel resistor of charge transfer (R_{ct}) and constant phase element (CPE) connected to its exponent. It can be observed that in Fig. 5, the total impedance in the recorded Nyquist plots increases with an increase of the inhibitor concentration. These plots are fitted to a circuit model using Gamry Analyst software, and the fitted values are listed in Table 4. Because the impedance of the inhibited mild steel increases with an increase in the **MPC** concentrations, the inhibition efficiency increases. The inhibition efficiency (E_{EIS}%) was calculated according to Eq. (6):

$$\mathbf{E=(1-R^{\circ}_{ct}/ R_{ct})x100} \qquad \mathbf{(6)}$$

In this equation, R_{ct} and R°_{ct} are the charge transfer resistance with and without the **MPC**, respectively.

The calculated double-layer capacitance values, C_{dl}, derived from the CPE parameters according to Eq. (7) are listed in Table 4 [27]:

$$C_{dl} = (AR^{1-n}{}_{ct})^{1/n} \quad (7)$$

In general, the values of the double-layer capacitance, C_{dl}, decreased in the presence of inhibitor. The decrease in C_{dl} is likely due to a decrease in the local dielectric constant and/or an increase in the thickness of a protective layer at the electrode surface, which would therefore enhance the corrosion resistance of the studied mild steel in a 1 M HCl solution at 308K.

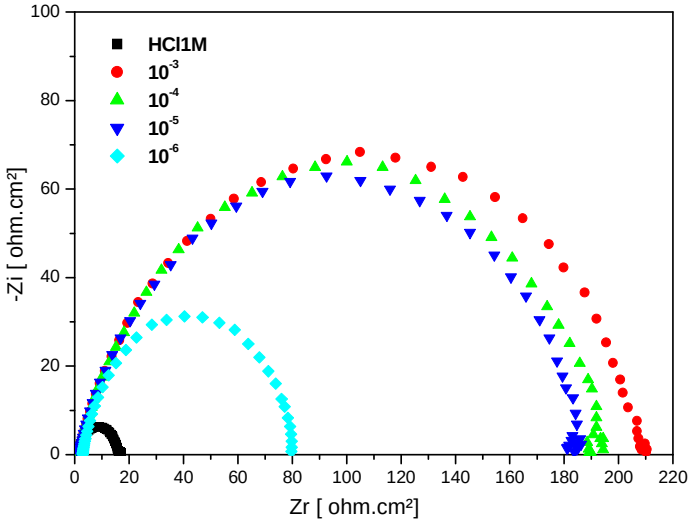

Figure 5: Nyquist plots for mild steel in 1 M HCl at 308K in the absence and presence of various concentrations of MPC

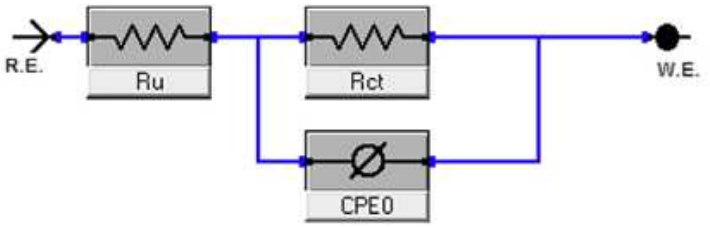

Figure 6: Electrical equivalent circuit model used for the modeling metal/solution

Table 4. Fitted impedance parameters of mild steel in 1 M HCl in the absence and the presence of different concentrations of MPC at 308k

Inhibitor	C_{inh} (M)	Rct (ohm .cm^2)	Ru (ohm.cm^2)	CPE0 (ohm^{-1} s^{n}cm^{-2})	n	Cdl (µF/cm^2)	E_{EIS} (%)
''MPC''	HCl 1M	14.50	1.93	193.87	0.886	200	--
	10^{-6}	79	2.54	133.96	0.819	64.20	82
	10^{-5}	182	1.55	116.52	0.793	55.15	92
	10^{-4}	194	1.55	110.41	0.827	51.67	93
	10^{-3}	209	1.57	103.14	0.814	48.94	**93**

3.3.4. Potential of zero charge (pzc)

Potential of zero charge is of a fundamental importance in surface science, which is a concept relating to the phenomenon of adsorption, and describing the condition when the electric charge density on a surface is zero. The surface charge of metal can be determined by the position of open circuit potential in respect to the respective pzc [28]. For this purpose, the electrochemical impedance measurements were applied at different potentials and a plot of C_{dl} versus applied potential was obtained. The plot corresponding to 1h of exposure time was given in Fig. 7.

In Fig. 7 the minimum C_{dl} was seen at -494 mV (Ag/AgCl) which can be named the pzc of mild steel in 10^{-3}M **MPC** containing 1 M HCl solution. The Eocp of mild steel in the same conditions was -0.464 V (Ag/AgCl). It is more positive than pzc, and this indicate positively charged mild steel surface. Due to anodic dissolution of metal, the

mild steel surface has positive charge, so Cl^- ions should be first adsorbed onto the surface, in this condition **MPC** molecule may exist as the protonated form in acidic medium and they adsorb the surface via electrostatic interactions(Fig. 8). Other sides, **MPC** molecules may on the mild steel surface via the unshared pair of electrons present on N and O atoms. Consequently, the corrosion rate of mild steel increases in the presence of **MPC** molecules.

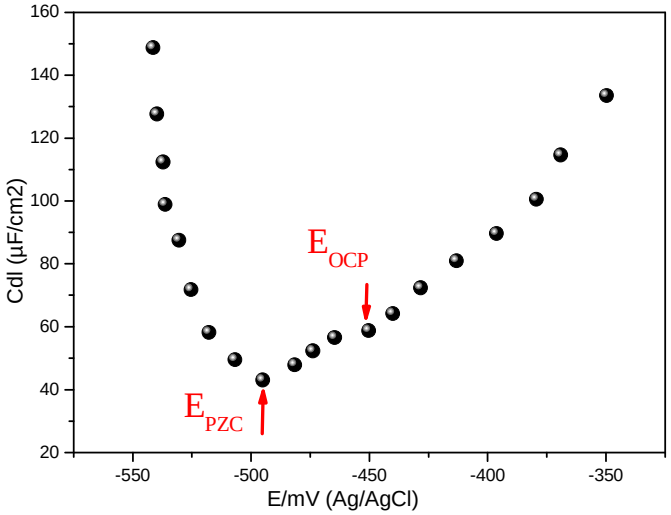

Figure 7. The plot of C_{dl} vs. applied potential in 1 M HCl containing 10^{-3}M MPC

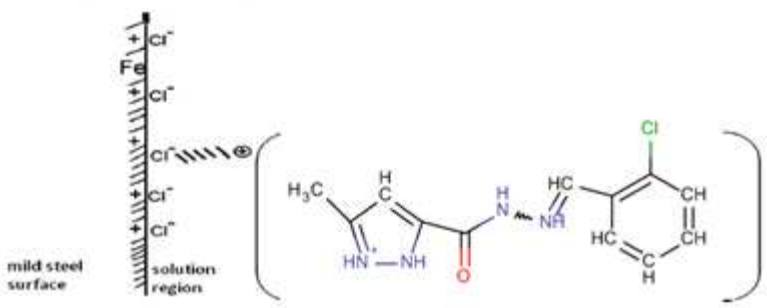

Figure. 8. The schematic illustration of the adsorption behaviour of the MPC on mild steel in 1 M HCl solution

3.4. Quantum chemical calculations

Quantum chemical computations were carried out by density function theory (DFT) with 6-31G (d, p) basis set for all atoms. All of the calculations were carried out with Gaussian 09W package [29].

Theoretical calculations were conducted in order to provide molecular-level understanding of the corrosion inhibition behavior of pyrazine derivative (**MPC**) and protonated structure **(p-MPC)** inhibitor. Fig.9 and 10 shows the optimized structure, HOMO and LUMO orbitals of (**MPC**) and **(p-MPC)** compounds. The quantum chemical parameters such as the energy of highest occupied molecular orbital (E_{HOMO}), the energy of lowest unoccupied molecular orbital (E_{LUMO}), energy gap (ΔE) between E_{HOMO} and E_{LUMO} and dipole moment (μ) were calculated and listed in Table 7. These parameters were found to be extremely important properties for interpreting the chemical reactivity of inhibitors with metal surfaces [30, 31].

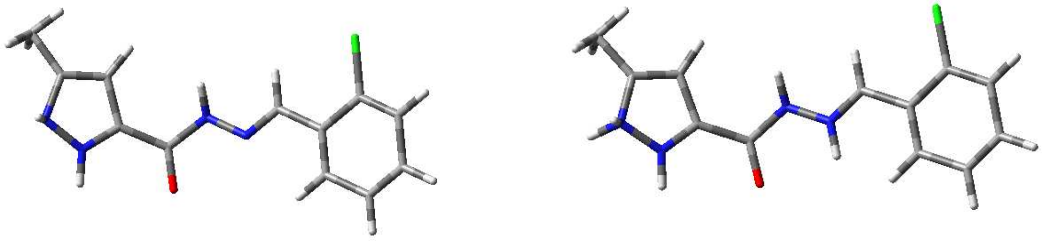

Figure9. Optimized structure of studied molecules obtained by B3LYP/6-31G(d,p) level

Table 7. Calculated quantum chemical parameters of the studied compounds

Quantum parameters	MPC	p-MPC
E_{HOMO} (eV)	-0.34930	-0.27976
E_{LUMO} (eV)	-0.19015	-0.1416
ΔEgap (eV)	0.15915	0.13816
Dipole moment μ (debye)	3.6641	6.3747

	HOMO	LUMO
Molecular **MPC**	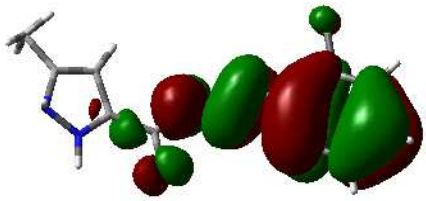	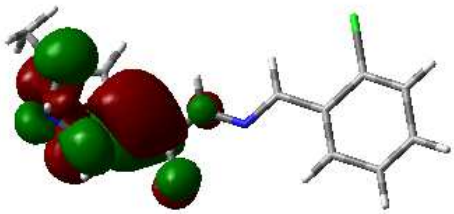
protonated structure **p-MPC**	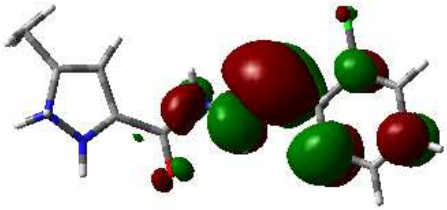	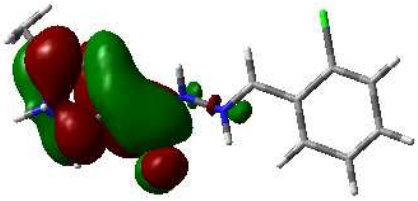

Figure 10. The frontier molecular orbital density distribution of MPC and p-MPC

The global molecular reactivity can be studied according to Fukui's theory of frontier molecular orbitals (FMO) in terms of interaction between the frontier orbitals, including HOMO and LUMO [32]. FMO theory is useful in predicting adsorption centers of the inhibitor molecules responsible of the interaction with surface metal atoms. The HOMO energy (E_{HOMO}) is often associated with the electron donating ability of the molecule; therefore, inhibitors with E_{HOMO} high values have a tendency to donate electrons to appropriate acceptor with low empty molecular orbital energy. Conversely, the LUMO energy (E_{LUMO}) indicates the electron accepting ability of the molecule, the lowest its value the higher the capability of accepting electrons. Similar relations were found between the rates of corrosion and ΔE ($\Delta E = E_{LUMO} - E_{HOMO}$) [33].

It can be seen from Fig. 10 that the HOMO and LUMO distribute around heteroatoms and aromatic rings. From Table 7, E_{HOMO} obeys the order: **p-MPC** > **MPC**, which is in full accordance with the order of inhibition efficiency. The main role in adsorption phenomena occurs on LUMO orbitals; the low E_{LUMO} is preferred because the feedback bonds are formed between d orbitals of metal and inhibitor. Formation of feedback bonds increases the chemical adsorption of inhibitor molecules on the metal surface and thus increases the inhibition efficiency [34]. The other important parameter is dipole moment, which can lead to increase of inhibition and can be related to the dipole–dipole interaction of molecules and metal surface [35]. In Table 7, **p-MPC** had higher dipole moment than the neutral molecule.

Consequently, calculated parameters showed that **MPC** was most probably protonated in acidic medium and **p-MPC** had better inhibition efficiency than the neutral molecule. All these calculations were correlated the experimental results.

CONCLUSION

The following results can be drawn from this study:

(1) MPC acts as a good inhibitor for the corrosion of mild steel in 1 M HCl and its inhibition efficiency is concentration dependent.
(2) The polarization measurements reveal that MPC behaves as a mixed-type inhibitor in 1 M HCl by acting on both anodic metal dissolution and cathodic hydrogen evolution reactions.
(3) The adsorption of the inhibitor on the surface of mild steel in 1 M HCl follows a Langmuir adsorption isotherm. The high value of adsorption equilibrium constant and negative value of standard free energy of adsorption suggested that MPC is strongly adsorbed on mild steel surface.

(4) The results obtained from the EIS showed that the corrosion inhibition efficiencies increased with an increase in inhibitor concentration.
(5) Theoretical calculations were in agreement with the experimental results and showed that MPC have interesting molecular structure for inhibiting the corrosion process. The protection ability of the MPC can be attributed to its molecular protonated structure.

REFERENCES

[1] H. Elmsellem, H. Nacer, F. Halaimia, A. Aouniti, I. Lakehal, A .Chetouani, S. S. Al-Deyab, I. Warad, R. Touzani, B. Hammouti. *Int. J. Electrochem. Sci*., **2014**, 9, 5328 – 5351
[2] R.W. Revie, H.H. Uhlig, *New Jersey.*, **2008**.
[3] N.O. Eddy, B.I. Ita, Q.S. AR, *J. Mol. Model*., **2011**, 17, 359–376.
[4] M. Bouayed, H. Rabaa, A. Srhiri, J.Y. Saillard, A. Ben Bachir. *Corros. Sci*., **1999**, 41, 501–517.
[5] M.A. Quraishi, R. Sardar, *Mater. Chem. Phys*., **2002**, 78, 425–431.
[6] E. Stupnišek-Lisac, S. Podbrscek, T. Soric, *J. Appl. Electrochem*., **1994**, 24, 779–784.
[7] F. Bentiss, M. Traisnel, L. Gengembre, M. Lagrenée, *Appl. Surf. Sci*., **2000**, 161, 194–202.
[8] A. Ouchrif, M. Zegmout, B. Hammouti, S. El-Kadiri, A. Ramdani, *Appl. Surf. Sci*., **2005**, 252, 339–344.
[9] G.K. Gomma, *Mater. Chem. Phys*., **1998**, 55, 241–246.
[10] M. Abdallah, M.M. El-Naggar, *Mater. Chem. Phys*., **2001,** 71, 291–298.
[11] M. Elayyachy, M. Elkodadi, A. Aouniti, A. Ramdani, B. Hammouti, F. Malek, A. Elidrissi, *Mater. Chem. Phys.*, **2005**, 93, 281–285.
[12] K. Tebbji, A. Aouniti, M. Benkaddour, H. Oudda, I. Bouabdallah, B. Hammouti, A. Ramdani, *Prog. Org. Coat.*, **2005**, 54, 170–174.
[13] M. Bouklah, A. Attayibat, S. Kertit, A. Ramdani, B. Hammouti, *Appl. Surf.Sci*., **2005**, 242, 399–406.
[14] M. Kissi, M. Bouklah, B. Hammouti, M. Benkaddour, *Appl. Surf. Sci*., **2005**, 252, 4190–4197.
[15] S.D. Deng, X.H. Li, H. Fu, *Corros. Sci*., **2011**, 53, 822–828.
[16] H. Elmsellem, H. Bendaha, A. Aouniti, A. Chetouani, M. Mimouni, A. Bouyanzer. Mor. J. Chem. **2014**, 2 (1), 1-9
[17] Z. GHAZI, M. RAMDANI, M. TAHRI, R. RMILI, H. ELMSELLEM, M. FAUCONNIER. *J. Mater. Environ. Sci.* **2015**, 6 (8), 2338-2345
[18] A. Zarrouk, H. Zarrok, R. Salghi, B. Hammouti,F. Bentiss, R. Touir, M. Bouachrine, *J. Mater. Environ. Sci.*, **2013**, 4 ,177.
[19] I. Langmuir, J. Am. *Chem. Soc*, **1947**, 39, 1848. 10.1021/ja02254a006
[20]Bensajjay F., Alehyen, S., El-Achouri ,M. S., Kertit,S., *Anti-Corros. Methods Mater*., ***2003***, 50, 402.
[21]Xu B., Liu, Y., Yin ,X.S., Yang, W.Z., Chen, Y. Z., *Corros. Sci*., **2013**, 74, 206.
[22] A.K. Sataphathy, G. Gunasekaran, S.C. Sahoo, K. Amit, P.V. Rodrigues, *Corros. Sci*., **2009**, 51, 2848–2856.
[23] M. Behpour, S.M. Ghoreishi, N. Soltani, M. Salavati-Niasari, *Corros. Sci*., **2009**, 51, 1073–1082.
[24] S. John, B. Joseph, K.K. Aravindakshan, A. Joseph, *Mater. Chem. Phys*., **2010**, 122, 374–379.
[25] G. Bereket, E. Hür, C.Ö. Retir, *J. Mol. Struct*. (*Theochem*)., **2002**, 578, 79–88.
[26] M. Lebrini, M. Lagrenée, H. Vezin, M. Traisnel, F. Bentiss, *Corros. Sci*. **2007**, 49, 2254–2269.
[27] F. Bentiss, M. Lebrini, M. Lagrenee, *Corros. Sci*, **2005**, 47, 2915.
[28] B. Dogru Mert, M.E. Mert, G. Kardas_, B. Yazıcı, *Corros. Sci.*, **2011**, 53, 4265–4272.
[29] H. Elmsellem, A. Aouniti, M. Khoutoul, A. Chetouani, B. Hammouti, N. Benchat, R.Touzani, M. Elazzouzi. *Journal of Chemical and Pharmaceutical Research*, **2014**, 6(4), 1216-1224
[30] M.M. Kabanda, L.C. Murulana, M. Ozcan, F. Karadag, I. Dehri, I.B. Obot, E.E. Ebenso, *Int. J. Electrochem. Sci.* , **2012**, 7, 5035.
[31] I.B. Obot, N.O. Obi-Egbedi, A.O. Eseola, *Ind. Eng. Chem. Res*., **2011**, 50, 2098.
[32] H. Elmsellem, N. Basbas, A. Chetouani, A. Aouniti, S. Radi, M. Messali, B. Hammouti, *Portugaliae. Electrochimica. Acta*, **2014**, 2,77.
[33] H. Elmsellem, A. Aouniti, Y. Toubi, H. Steli, M. Elazzouzi, S. Radi, B. Elmahi, Y. El Ouadi, A. Chetouani, B. Hammouti. *Der Pharma Chemica*, **2015**, 7, 353-364
[34] H. Elmsellem, M. H.Youssouf, A. Aouniti, T. Ben Hadda, A. Chetouani, B. Hammouti. *Russian Journal of Applied Chemistry*, **2014**, 87(6), 744−753
[35] H. Elmsellem, T. Harit, A. Aouniti, F. Malek, A. Riahi, A. Chetouani , and B. Hammouti. *Protection of Metals and Physical Chemistry of Surfaces*, **2015**, 51(5), 873–884